

Ghost condensation on the lattice

Attilio Cucchieri, Tereza Mendes and Antonio Mihara

*Instituto de Física de São Carlos,
Universidade de São Paulo,
C.P. 369, 13560-970, São Carlos, SP, Brazil*

We perform a numerical study of ghost condensation — in the so-called Overhauser channel — for $SU(2)$ lattice gauge theory in minimal Landau gauge. The off-diagonal components of the momentum-space ghost propagator $G^{cd}(p)$ are evaluated for lattice volumes $V = 8^4, 12^4, 16^4, 20^4, 24^4$ and for three values of the lattice coupling: $\beta = 2.2, 2.3, 2.4$. Our data show that the quantity $\phi^b(p) = \epsilon^{bcd}G^{cd}(p)/2$ is zero within error bars, being characterized by very large statistical fluctuations. On the contrary, $|\phi^b(p)|$ has relatively small error bars and behaves at small momenta as $L^{-2}p^{-z}$, where L is the lattice side in physical units and $z \approx 4$. We argue that the large fluctuations for $\phi^b(p)$ come from spontaneous breaking of a global symmetry and are associated with ghost condensation. It may thus be necessary (in numerical simulations at finite volume) to consider $|\phi^b(p)|$ instead of $\phi^b(p)$, to avoid a null average due to tunneling between different broken vacua. Also, we show that $\phi^b(p)$ is proportional to the Fourier-transformed gluon field components $\tilde{A}_\mu^b(q)$. This explains the L^{-2} dependence of $|\phi^b(p)|$, as induced by the behavior of $|\tilde{A}_\mu^b(q)|$. We fit our data for $|\phi^b(p)|$ to the theoretical prediction $(r/L^2 + v)/(p^4 + v^2)$, obtaining for the ghost condensate v an upper bound of about 0.058 GeV^2 . In order to check if v is nonzero in the continuum limit, one probably needs numerical simulations at much larger physical volumes than the ones we consider. As a by-product of our analysis, we perform a careful study of the color structure of the inverse Faddeev-Popov matrix in momentum space.

PACS numbers: 11.15.Ha, 12.38.Aw, 12.38.Gc, 14.80.-j

I. INTRODUCTION

The QCD vacuum is known to be highly non-trivial at low energies [1]. This non-trivial structure manifests itself through the appearance of vacuum condensates, i.e. vacuum expectation values of certain local operators. In perturbation theory these condensates vanish, but in the SVZ-sum-rule approach [2, 3] they are included as a parametrization of non-perturbative effects in the evaluation of phenomenological quantities. Of course, the local operators considered must be gauge invariant in order to be added as higher-dimension operators (higher twists) to the usual perturbative expansion of physical quantities. The two main such operators are $\alpha_s F_{\mu\nu} F^{\mu\nu}$ and $m_q \bar{\psi}_q \psi_q$; their vacuum expectation values are the so-called gluon and quark condensates. Both of these operators have mass dimension four.

In recent years, (gauge-dependent) condensates of mass dimension two have also received considerable attention [4, 5, 6, 7, 8, 9, 10, 11, 12, 13, 14, 15, 16, 17, 18, 19, 20, 21, 22, 23, 24, 25, 26, 27, 28, 29, 30, 31, 32, 33, 34]. In particular, the gauge condensate $\langle A_\mu^b A_\mu^b \rangle$ has been largely studied, since it should be sensitive to topological structures such as monopoles [4, 5]. Thus, this parameter could play an important role in the quark-confinement scenario through monopole condensation [35, 36, 37]. Moreover, the existence of a gauge condensate would imply a dynamical mass generation for the gluon and ghost fields. This result has already been obtained in various gauges [16, 17, 21, 31, 33], but clearly, since the operator $A_\mu^b A_\mu^b$ is not gauge invariant, it is difficult to assign

a physical interpretation to the condensate $\langle A_\mu^b A_\mu^b \rangle$. Recently, evidence that the expectation value $\langle A_\mu^b A_\mu^b \rangle$ may be gauge independent was presented in [24, 25, 26, 34]. At the same time, the authors of Refs. [4, 5] have shown that the minimal value of $\langle A_\mu^b A_\mu^b \rangle$ (on each gauge orbit) has a gauge-invariant meaning. Let us note that this minimal value is achieved by considering absolute minima in the minimal Landau gauge, i.e. for configurations belonging to the so-called (Landau) fundamental modular region [38].

Other vacuum condensates of mass dimension two considered by several groups are the ghost condensates $\langle f^{bcd} \bar{\eta}^c \eta^d \rangle$, $\langle f^{bcd} \eta^c \eta^d \rangle$ and $\langle f^{bcd} \bar{\eta}^c \bar{\eta}^d \rangle$. These condensates were first introduced in $SU(2)$ gauge theory in maximally Abelian gauge (MAG) [7, 10, 27, 32, 39, 40, 41]. More recently, the same condensates have been studied in other gauges [6, 8, 9, 13, 28, 30], such as the Curci-Ferrari and the Landau gauges. In all cases it was found that the ghost condensates are related to the breakdown of a global $SL(2, R)$ symmetry [6, 42]. In MAG the diagonal and off-diagonal components of the ghost propagators are modified [7, 27] by ghost condensation. Similar results have been obtained in other gauges [13, 30]. In particular, in Landau gauge it was shown [13] that the off-diagonal (anti-symmetric) components of the ghost propagator $G^{cd}(p)$ — or, equivalently, the quantity $\phi^b(p)$ — are proportional to the ghost condensate v . In the same reference it is argued that the breaking of the global $SU(N_c)$ color symmetry, related to this non-zero expectation value for $G^{cd}(p)$, may occur only in the unphysical sector of the Hilbert space and therefore should not be (explicitly) observable in the physical subspace. Very re-

cently [23], the effects of the ghost condensate $\langle f^{bcd}\bar{\eta}^c\eta^d \rangle$ and of the gauge condensate $\langle A_\mu^b A_\mu^b \rangle$ have been considered together for the $SU(2)$ case in Landau gauge, showing that ghost condensation induces a splitting in the gluon mass related to the gauge condensate.

It is interesting that the existence of different ghost condensates has an analogue in the theory of superconductivity [13]. In particular, the condensates $\langle f^{bcd}\bar{\eta}^c\eta^d \rangle$ and $\langle f^{bcd}\bar{\eta}^c\bar{\eta}^d \rangle$ correspond to the so-called BCS effect [43, 44], in which particle-particle and hole-hole pairing occur, while the condensate $\langle f^{bcd}\bar{\eta}^c\eta^d \rangle$ is analogous to the Overhauser effect [45], in which particle-hole pairing occurs. Also, in the Curci-Ferrari gauge, both effects have to be considered [13] in order to obtain an action invariant under the so-called Nakanishi-Ojima (NO) algebra. It is this NO algebra that includes an $SL(2, R)$ sub-algebra.

Finally, a mixed gluon-ghost condensate of mass dimension two has also been studied by several authors [10, 12, 18, 20, 29, 30], using various gauges. This mixed condensate is of particular interest when considering interpolating gauges [18]. Indeed, it allows to generalize and relate results obtained in different gauges for the gauge condensate $\langle A_\mu^b A_\mu^b \rangle$ and the ghost condensates. Moreover, in MAG this mixed condensate would induce a dynamic mass for the off-diagonal gluons [20], giving support to the Abelian-dominance scenario [46, 47, 48, 49]. Thus, the various gauge and ghost condensates could all play an important role in the dual superconducting scenario of quark confinement [50, 51, 52], being related to monopole condensation and to Abelian dominance.

Possible effects of the gauge condensate $\langle A_\mu^b A_\mu^b \rangle$ on propagators and vertices (in Landau gauge) have been studied through lattice simulations in Refs. [53, 54, 55, 56, 57, 58, 59], yielding $\langle A_\mu^b A_\mu^b \rangle \approx 3 \text{ GeV}^2$. On the other hand, the ghost condensate has been considered numerically only in Ref. [60], for minimal Landau gauge in the Overhauser channel, both for the $SU(2)$ and $SU(3)$ cases. The authors find that the color off-diagonal anti-symmetric components of the ghost propagators are identically zero, while the symmetric components are zero within error bars, but have fluctuations proportional to $N^{-2}\hat{p}^{-4}$, where \hat{p} is the lattice momentum and N is the lattice side.

In this paper we carry out a thorough investigation of ghost condensation in the Overhauser channel for pure $SU(2)$ Yang-Mills theory in minimal Landau gauge. In particular, we evaluate numerically the off-diagonal components of the ghost propagator $G^{cd}(p)$ as a function of the momentum p . We find that $\langle \phi^b(p) \rangle = \epsilon^{bcd} \langle G^{cd}(p) \rangle / 2$ is zero within error bars, but with large fluctuations. On the other hand, if we consider the absolute value of $\phi^b(p)$, we find that $\langle |\phi^b(p)| \rangle$ behaves at small momenta as $L^{-2}p^{-z}$, where L and p are, respectively, the lattice side and the momentum in physical units and $z \approx 4$. As we will show [see Eq. (65)], the sign of $\phi^b(p)$ is related to the

sign of the Fourier-transformed gluon field components $\bar{A}(q)$. At the same time, one should recall that a nonzero value for $\phi^b(p)$ is related to the spontaneous breaking of a global $SL(2, R)$ symmetry [6, 42]. Thus, the situation here is similar to the one encountered in numerical studies of spin systems with nonzero spontaneous magnetization, in the absence of an external magnetic field. Indeed, since spontaneous symmetry breaking can occur only in the thermodynamic limit, when performing numerical simulations at finite volume one always finds (after sufficiently many Monte Carlo steps) a null magnetization for all nonzero temperatures [102]. This is due to the fact that, at finite volume, the probability that the system may pass from a state near a broken vacuum to a state near a different broken vacuum is always nonzero. To avoid this problem, the usual solution is to consider the absolute value of the magnetization or the root mean square order parameter, i.e. $\langle |\vec{M}| \rangle$ or $\langle \vec{M}^2 \rangle^{1/2}$. The results obtained using these two quantities do not agree at finite volume, but they produce the same infinite-volume-limit result [61, Fig. 2.13]. Alternatively, one can also simulate spin models with an external magnetic field H [63] and then consider the limit $H \rightarrow 0$. In our case, one could set the sign of $\phi^b(p)$ by adding to the action a constant external chromo-magnetic field coupled to the gluon field or, equivalently, one can fix this sign by a global gauge transformation. This is analogous to using a global rotation in a spin system in order to fix a direction for the magnetization. In all cases, i.e. introducing an external magnetic field, making a global transformation, or taking the absolute value of the order parameter, one explicitly breaks the global symmetry of the system choosing one of the (equivalent) possible vacua. In the present work we will consider the absolute value of $\phi^b(p)$, but we also describe (in Section III A) a possible global gauge transformation to select a unique broken vacuum.

Another indication of spontaneous symmetry breaking is the direct investigation of the statistical distribution of the order parameter, obtained from histograms of the produced Monte Carlo data. Let us recall that, given a random variable x with a Gaussian distribution $e^{-x^2/(2a)}/\sqrt{2\pi a}$, corresponding to a null mean value and a standard deviation \sqrt{a} , one finds that the variable $|x|$ has mean value $\sqrt{2a/\pi}$ and standard deviation $\sqrt{(\pi-2)a/\pi} \approx 0.75 \langle |x| \rangle$. Thus, if one evaluates the quantity x and finds that its average is null within error bars while $|x|$ has a relatively small error, one should conclude that the data for x do not correspond to a Gaussian distribution and that the fluctuations observed are not just statistical ones, since in this case they should be large also when considering the absolute value of x . This is indeed what happens for the magnetization of a spin system in the broken (low-temperature) phase, as can be easily verified by comparing a histogram of the data with a Gaussian distribution. This is true both for discrete symmetries — as in the Ising model, for which the distribution of the magnetization has two

peaks [61, 62] — and for continuous symmetries, such as for the three-dimensional $O(N)$ -symmetric nonlinear σ -models. In this case (see Fig. 1), the shape of the statistical distribution of the data is similar to a Gaussian, but with a larger width around the peak of the curve. Moreover, the width becomes larger as the temperature of the system decreases. On the contrary, in the unbroken phase, the histogram of the data is indeed a Gaussian distribution (see again Fig. 1). Note that a simple way of evaluating the Gaussian character of a distribution [61] is to consider the so-called Binder cumulant

$$U = 1 - \frac{\langle x^4 \rangle}{3 \langle x^2 \rangle^2} \quad (1)$$

for the order parameter x . In the infinite-volume limit this quantity is zero if x has a Gaussian distribution, i.e. in the unbroken phase, and is equal to $2/3$ if the distribution of x has two peaks, as in the broken phase of the Ising model. Thus, in general one should expect $U \neq 0$ in the broken phase, where the value of U depends on the distribution of x . In the case of the ghost condensate, based on the discussion above, we argue that the occurrence of large fluctuations for $\phi^b(p)$ but not for $|\phi^b(p)|$ implies that the global symmetry $SL(2, R)$ is indeed broken. We will analyze the statistical distribution for $\phi^b(p)$ in Section V.

As mentioned above, we show in Eq. (65) that the quantity $\phi^b(p)$ is proportional to the Fourier-transformed

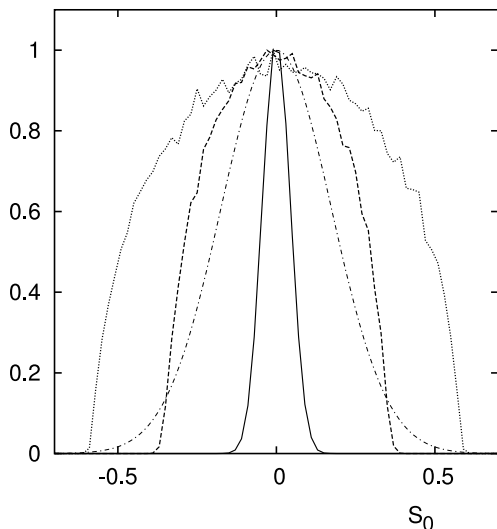


FIG. 1: Histograms for the first component of the magnetization in the $3d$ $O(4)$ nonlinear σ -model. Solid, dashed and dotted lines correspond respectively to inverse temperature $\beta = 0.9$ (in the symmetric phase), $\beta = 0.98$ and $\beta = 1.2$ (both in the broken phase). In the three cases we considered 100,000 independent configurations. For comparison, we show (dot-dashed line) a Gaussian with the same mean and variance as the case $\beta = 0.98$.

gluon field $\tilde{A}(q)$. This dependence can explain the $1/L^2$ behavior of $\phi^b(p)$ as induced by $\tilde{A}(q)$. Indeed, for $q = 0$ it was proven [64] that $\langle |\tilde{A}(0)| \rangle$ goes to zero in the infinite-volume limit at least as fast as $1/L$. Furthermore, in Section V we verify from our data that $|\tilde{A}^b(q)|$ behaves as $1/L^2$. We stress that this result does not imply that $|\phi^b(p)|$ is zero at infinite volume, because $\langle |\phi^b(p)| \rangle$ is not simply proportional to $\langle |\tilde{A}^b(q)| \rangle$, as can be seen in Eq. (87).

The paper is organized as follows. In Section II we review the definition of the Faddeev-Popov operator — from which we obtain the ghost propagator — on the lattice (for the minimal Landau gauge) and in the continuum (in Landau gauge) for a general $SU(N_c)$ gauge group. In Section III we define $\phi^b(p)$ and show that it is proportional to the Fourier-transformed gluon field $\tilde{A}(q)$. In that Section we also discuss how to find a global gauge transformation that changes the sign of $\phi^b(p)$. Our numerical simulations are explained in Section IV and the results are reported in Section V. Let us stress that, as a by-product of our analysis, we also present a careful study of the color structure of the inverse Faddeev-Popov matrix in momentum space. At the same time, we consider the infinite-volume limit for the momentum-space gluon field components $\tilde{A}(q)$. Finally, in Section VI we draw our conclusions.

II. THE LANDAU FADDEEV-POPOV OPERATOR

Let us recall that, on a d -dimensional lattice, the (minimal) Landau gauge is obtained, in the $SU(N_c)$ case, by considering the functional

$$\begin{aligned} \mathcal{E}_U[g] &= -\frac{1}{dV} \sum_x \sum_\mu \Re \frac{\text{Tr}}{N_c} [g(x) U_\mu(x) g^\dagger(x + e_\mu)] \quad (2) \\ &= -\frac{1}{dV} \sum_x \sum_\mu \frac{\text{Tr}}{2N_c} [g(x) U_\mu(x) g^\dagger(x + e_\mu) \\ &\quad + g(x + e_\mu) U_\mu^\dagger(x) g^\dagger(x)]. \quad (3) \end{aligned}$$

Here $\{U_\mu(x)\}$ is a given (*i.e.* fixed) thermalized lattice configuration, V is the lattice volume and the gauge-fixing condition is imposed by finding a gauge transformation $\{g(x)\}$ that brings this functional to a minimum. Both the link variables $U_\mu(x)$ and the gauge transformation matrices $g(x)$ are elements of the $SU(N_c)$ group (in the fundamental $N_c \times N_c$ representation). Also, $\mathbb{1}$ indicates the identity matrix and e_μ is a positive unit vector in the μ direction. Note that we set the lattice spacing a equal to 1 in order to simplify the notation.

Let us also consider [38, 65] a one-parameter subgroup $g(\tau; x) = \exp [i \tau \gamma^b(x) \lambda^b]$, where τ is a real parameter, λ^b are the $N_c^2 - 1$ traceless Hermitian generators of $SU(N_c)$ (also in the fundamental representation), the

components of $\gamma^b(x)$ are real and the sum over the color index b is understood. We consider generators λ^b normalized such that $\text{Tr}(\lambda^b \lambda^c) = 2\delta^{bc}$. In the $SU(2)$ case these generators are the three Pauli matrices σ^b . Using this one-parameter subgroup we can regard \mathcal{E}_U as a function of the parameter τ . Its first derivative with respect to τ calculated at $\tau = 0$ is given by

$$\mathcal{E}'(0) = \frac{2}{dV N_c} \sum_x \gamma^b(x) (\nabla \cdot A^b)(x). \quad (4)$$

Here

$$(\nabla \cdot A^b)(x) = \sum_\mu A_\mu^b(x) - A_\mu^b(x - e_\mu) \quad (5)$$

is the lattice divergence of the gluon field $A_\mu^b(x)$, defined as

$$A_\mu^b(x) = \frac{1}{2} \text{Tr} [A_\mu(x) \lambda^b] \quad (6)$$

with [103]

$$A_\mu(x) = \frac{1}{2i} [U_\mu(x) - U_\mu^\dagger(x)]_{\text{traceless}} \quad (7)$$

or, equivalently,

$$A_\mu(x) = \frac{1}{2i} [U_\mu(x) - U_\mu^\dagger(x)] - \mathbb{1} \frac{\text{Tr}}{2i N_c} [U_\mu(x) - U_\mu^\dagger(x)]. \quad (8)$$

The last term in the above equation is zero in the $SU(2)$ case and the definition of the lattice gluon field simplifies to

$$A_\mu(x) = \frac{1}{2i} [U_\mu(x) - U_\mu^\dagger(x)]. \quad (9)$$

Then, one can write the $SU(2)$ link variables $U_\mu(x)$ as

$$U_\mu(x) = U_\mu^0(x) \mathbb{1} + i A_\mu^b(x) \sigma^b \quad (10)$$

with

$$[U_\mu^0(x)]^2 + \sum_b [A_\mu^b(x)]^2 = 1. \quad (11)$$

Also, note that, since the generators λ^b are traceless, the term proportional to the identity matrix $\mathbb{1}$ in Eq. (8) does not contribute to $A_\mu^b(x)$ [see Eq. (6)]. Thus, for any $N_c \geq 2$ we find

$$A_\mu(x) = \lambda^b A_\mu^b(x) = \frac{\lambda^b}{2} \text{Tr} [A_\mu(x) \lambda^b] \quad (12)$$

$$= \frac{\lambda^b}{4i} \text{Tr} \{ [U_\mu(x) - U_\mu^\dagger(x)] \lambda^b \} \quad (13)$$

$$= \frac{\lambda^b}{2} \text{Im Tr} [U_\mu(x) \lambda^b]. \quad (14)$$

If $\{U_\mu(x)\}$ is a stationary point of $\mathcal{E}(\tau)$ at $\tau = 0$ then we have $\mathcal{E}'(0) = 0$ for every $\{\gamma^b(x)\}$. This implies [see Eq. (4)]

$$(\nabla \cdot A^b)(x) = 0 \quad (15)$$

for any x and b , which is the lattice formulation of the usual Landau gauge-fixing condition in the continuum. Let us recall that the continuum gluon field $A_\mu^{(c)}(x)$ [104] is related to the link variables $U_\mu(x)$ by the relation

$$U_\mu(x) = \exp [i a g_0 A_\mu^{(c)}(x)], \quad (16)$$

where g_0 is the lattice bare coupling constant. This yields [105]

$$A_\mu(x) = a g_0 A_\mu^{(c)}(x) + \mathcal{O}(a^3). \quad (17)$$

Finally, using

$$\nabla_\mu = a \partial_\mu + \mathcal{O}(a^2) \quad (18)$$

we obtain from Eq. (15) the result

$$(\partial \cdot A^b)(x) = \mathcal{O}(a). \quad (19)$$

Still considering the one-parameter subgroup $g(\tau; x)$ and the general $SU(N_c)$ case we can evaluate the second derivative of $\mathcal{E}(\tau)$ at $\tau = 0$. We obtain

$$\mathcal{E}''(0) = \frac{2}{dV N_c} \sum_{x,y} \sum_{b,c} \gamma^b(x) \mathcal{M}_U^{bc}(x,y) \gamma^c(y) \quad (20)$$

$$= \frac{2}{dV N_c} \sum_x \sum_b \gamma^b(x) (\mathcal{M}_U \gamma)^b(x), \quad (21)$$

with [38]

$$\begin{aligned} (\mathcal{M}_U \gamma)^b(x) &= \sum_\mu \Gamma_\mu^{bc}(x) [\gamma^c(x) - \gamma^c(x + e_\mu)] \\ &\quad + \Gamma_\mu^{bc}(x - e_\mu) [\gamma^c(x) - \gamma^c(x - e_\mu)] \\ &\quad + f^{bdc} [A_\mu^d(x) \gamma^c(x + e_\mu) \\ &\quad - A_\mu^d(x - e_\mu) \gamma^c(x - e_\mu)]. \end{aligned} \quad (22)$$

Here $\mathcal{M}_U^{bc}(x,y)$ is the lattice Faddeev-Popov matrix and f^{bcd} are the (anti-symmetric) structure constants defined by $[\lambda^b, \lambda^c] = 2i f^{bcd} \lambda^d$. We also have [38]

$$\Gamma_\mu^{bc}(x) = \text{Tr} \left[\left\{ \frac{\lambda^b}{2}, \frac{\lambda^c}{2} \right\} \frac{U_\mu(x) + U_\mu^\dagger(x)}{2} \right]. \quad (23)$$

In the $SU(2)$ case [69] one finds $\Gamma_\mu^{bc}(x) = \delta^{bc} \text{Tr} U_\mu(x)/2$ and $f^{bcd} = \epsilon^{bcd}$, where ϵ^{bcd} is the completely anti-symmetric tensor. In this case, Eqs. (21) and (22) agree

with Eq. (11) of Ref. [65]. Note that, by using Eqs. (5) and (15), we can re-write Eq. (22) as

$$\begin{aligned}
(\mathcal{M}_U \gamma)^b(x) &= \sum_{\mu} \Gamma_{\mu}^{bc}(x) [\gamma^c(x) - \gamma^c(x + e_{\mu})] \\
&+ \Gamma_{\mu}^{bc}(x - e_{\mu}) [\gamma^c(x) - \gamma^c(x - e_{\mu})] \\
&+ f^{bdc} \{A_{\mu}^d(x) [\gamma^c(x + e_{\mu}) + \gamma^c(x)] \\
&- A_{\mu}^d(x - e_{\mu}) [\gamma^c(x - e_{\mu}) + \gamma^c(x)]\}. \quad (24)
\end{aligned}$$

We then obtain

$$\begin{aligned}
(\mathcal{M}_U \gamma)^b(x) &= \sum_{\mu} (D_{\mu} \gamma)^b(x) - (D_{\mu} \gamma)^b(x - e_{\mu}) \quad (25) \\
&= (\nabla \cdot D_{\mu} \gamma)^b(x), \quad (26)
\end{aligned}$$

where we used the definition (5) of the lattice divergence and

$$\begin{aligned}
(D_{\mu} \gamma)^b(x) &= \Gamma_{\mu}^{bc}(x) [\gamma^c(x) - \gamma^c(x + e_{\mu})] \\
&+ f^{bdc} A_{\mu}^d(x) [\gamma^c(x + e_{\mu}) + \gamma^c(x)] \quad (27)
\end{aligned}$$

is the (negative of the) lattice covariant derivative [38] applied to $\gamma^c(x)$. Equivalently, we can write Eq. (22) as

$$\begin{aligned}
(\mathcal{M}_U \gamma)^b(x) &= \sum_{\mu} \Gamma_{\mu}^{bc}(x) [\gamma^c(x) - \gamma^c(x + e_{\mu})] \\
&+ \Gamma_{\mu}^{bc}(x - e_{\mu}) [\gamma^c(x) - \gamma^c(x - e_{\mu})] \\
&+ f^{bdc} \{A_{\mu}^d(x) [\gamma^c(x + e_{\mu}) - \gamma^c(x)] \\
&- A_{\mu}^d(x - e_{\mu}) [\gamma^c(x - e_{\mu}) - \gamma^c(x)]\} \quad (28)
\end{aligned}$$

and it is evident that the second derivative $\mathcal{E}''(0)$ is null if the vector $\gamma^c(x)$ is constant, i.e. the Faddeev-Popov matrix has a trivial null eigenvalue corresponding to a constant eigenvector. It is also clear that, if $\{U_{\mu}(x)\}$ is a local minimum of $\mathcal{E}(\tau)$ at $\tau = 0$, then the matrix \mathcal{M}_U is positive definite (in the subspace orthogonal to the space of constant vectors).

Let us recall that, in the continuum, if one considers a gauge-fixing condition $[F(A^g)]^b(x) = 0$ and the gauge transformation $g(x) = e^{i g_0 \theta^b(x) \lambda^b}$, the Faddeev-Popov operator can be determined using the expansion

$$\begin{aligned}
[F(A^g)]^b(x) &= [F(A)]^b(x) \\
&+ \int d^4 y \sum_c \mathcal{M}^{bc}(x, y) \theta^c(y) + \dots \quad (29)
\end{aligned}$$

In the Landau case one has $[F(A)]^b(x) = (\partial_{\mu} A_{\mu}^b)(x)$, giving

$$\mathcal{M}^{bc}(x, y) = -\partial_{\mu} D_{\mu}^{bc}(x) \delta(x - y) \quad (30)$$

$$= -D_{\mu}^{bc}(x) \partial_{\mu} \delta(x - y) \quad (31)$$

$$= -[\delta^{bc} \partial_{\mu} - 2 g_0 f^{bdc} A_{\mu}^d(x)] \partial_{\mu} \delta(x - y) \quad (32)$$

$$= -[\delta^{bc} \partial_{\mu} + 2 g_0 f^{bcd} A_{\mu}^d(x)] \partial_{\mu} \delta(x - y), \quad (33)$$

where $D_{\mu}^{bc}(x)$ is the (continuum) covariant derivative. Note that, with our normalization for the generators λ^b , we have that $2 A_{\mu}^d(x)$ is the standard continuum gluon field.

Clearly, we can expand Eq. (16) in the limit $a \rightarrow 0$ as

$$U_{\mu}^0(x) = \mathbb{1} + i a g_0 A_{\mu}(x) + \mathcal{O}(a^2), \quad (34)$$

yielding

$$\Gamma_{\mu}^{bc}(x) \approx \delta^{bc} + \mathcal{O}(a^2). \quad (35)$$

Also, after Taylor expanding the vectors $\gamma^b(x \pm e_{\mu}) = \gamma^b(x \pm a e_{\mu})$ to order a^2 in Eq. (22), one obtains

$$a^{-2} \mathcal{M}_U^{bc}(x, y) = \mathcal{M}^{bc}(x, y) + \mathcal{O}(a), \quad (36)$$

with $\mathcal{M}^{bc}(x, y)$ given in Eq. (32). At the same time, from Eq. (27) we find the relation between the lattice and the continuum expressions for the covariant derivative

$$D_{\mu}^{bc}(x) = -a D_{\mu}^{(c)bc}(x) + \mathcal{O}(a^2) \quad (37)$$

and it is immediate to obtain Eq. (30), using Eqs. (26) and (18).

III. THE GHOST CONDENSATE

Let us note that the lattice Faddeev-Popov matrix $\mathcal{M}_U^{bc}(x, y)$ is symmetric with respect to the exchange $(b, x) \leftrightarrow (c, y)$. Indeed, from Eq. (22) we can write [70]

$$\begin{aligned}
\mathcal{M}_U^{bc}(x, y) &= \sum_{\mu} \Gamma_{\mu}^{bc}(x) [\delta_{x, y} - \delta_{x+e_{\mu}, y}] \\
&+ \Gamma_{\mu}^{bc}(x - e_{\mu}) [\delta_{x, y} - \delta_{x-e_{\mu}, y}] \\
&+ f^{bdc} [A_{\mu}^d(x) \delta_{x+e_{\mu}, y} \\
&- A_{\mu}^d(x - e_{\mu}) \delta_{x-e_{\mu}, y}] \quad (38)
\end{aligned}$$

and it is straightforward to verify that $\mathcal{M}_U^{bc}(x, y) = \mathcal{M}_U^{cb}(y, x)$. Moreover, using the fact that the inverse of a symmetric matrix is also symmetric, we have that the same property is satisfied by the inverse matrix

$$G^{bc}(x, y) = (\mathcal{M}_U^{-1})^{bc}(x, y). \quad (39)$$

Let us recall that, if a matrix $M^{bc}(x, y)$ has two different sets of indices, it can always be decomposed as

$$\begin{aligned}
M^{bc}(x, y) &= M_{ss}^{bc}(x, y) + M_{sa}^{bc}(x, y) \\
&+ M_{as}^{bc}(x, y) + M_{aa}^{bc}(x, y), \quad (40)
\end{aligned}$$

where the sub-scripts s and a indicate symmetry and anti-symmetry with respect to the color or to the space-time indices (in this order). Furthermore, if the matrix $M^{bc}(x, y)$ is symmetric with respect to the exchange

$(b, x) \leftrightarrow (c, y)$, as in the case of the Landau Faddeev-Popov matrix \mathcal{M}_U , then this decomposition simplifies to

$$M^{bc}(x, y) = M_{ss}^{bc}(x, y) + M_{aa}^{bc}(x, y). \quad (41)$$

Indeed, for the Faddeev-Popov matrix $\mathcal{M}_U^{bc}(x, y)$ [see Eq. (38)] we have that the terms containing $\Gamma_\mu^{bc}(x)$ are symmetric under the exchange $b \leftrightarrow c$ and under the exchange $x \leftrightarrow y$. At the same time, the terms containing f^{bcd} are anti-symmetric in the color indices and in the space-time coordinates x and y . Thus, in the $SU(2)$ case, we can write [see Eqs. (22) and (23)]

$$\mathcal{M}_U^{bc}(x, y) = \delta^{bc} \mathcal{S}(x, y) - f^{bcd} \mathcal{A}^d(x, y) \quad (42)$$

with $\mathcal{S}(x, y) = \mathcal{S}(y, x)$ and $\mathcal{A}^d(x, y) = -\mathcal{A}^d(y, x)$, corresponding to the decomposition (41). Note that the above formula also holds in the continuum [see Eq. (33)] for any $N_c \geq 2$. Then, the inverse Faddeev-Popov matrix is given by

$$\begin{aligned} (\mathcal{M}_U^{-1})^{bc}(x, y) &= \{ \delta^{be} \mathcal{S}(x, w) [\delta^{ec} \delta_{w, y} \\ &\quad - f^{ecd} \mathcal{S}^{-1}(w, z) \mathcal{A}^d(z, y)] \}^{-1}, \quad (43) \end{aligned}$$

where the sum over repeated indices is understood. This implies that the inverse matrix $G^{bc}(x, y)$ defined in Eq. (39) above can be evaluated using [106]

$$\begin{aligned} G^{bc}(x, y) &= \delta^{bc} \mathcal{S}^{-1}(x, y) \\ &\quad + f^{bcd} \mathcal{S}^{-1}(x, z) \mathcal{A}^d(z, w) \mathcal{S}^{-1}(w, y) \\ &\quad + [f^{bdh} f^{dcj} \mathcal{S}^{-1}(x, z) \mathcal{A}^h(z, s) \mathcal{S}^{-1}(s, r) \\ &\quad \quad \mathcal{A}^j(r, w) \mathcal{S}^{-1}(w, y)] + \dots \quad (44) \end{aligned}$$

We can also write

$$G^{bc}(x, y) = G_e^{bc}(x, y) + G_o^{bc}(x, y). \quad (45)$$

Here

$$\begin{aligned} G_e^{bc}(x, y) &= \delta^{bc} \mathcal{S}^{-1}(x, y) + f^{bdh} f^{dcj} [\\ &\quad \mathcal{S}^{-1} \mathcal{A}^h \mathcal{S}^{-1} \mathcal{A}^j \mathcal{S}^{-1}] (x, y) + \dots \quad (46) \end{aligned}$$

includes all terms of Eq. (44) with an even number of factors $\mathcal{A}^d(z, w)$ and

$$\begin{aligned} G_o^{bc}(x, y) &= f^{bcd} [\mathcal{S}^{-1} \mathcal{A}^d \mathcal{S}^{-1}] (x, y) + f^{bdh} f^{dej} f^{ecl} [\\ &\quad \mathcal{S}^{-1} \mathcal{A}^h \mathcal{S}^{-1} \mathcal{A}^j \mathcal{S}^{-1} \mathcal{A}^l \mathcal{S}^{-1}] (x, y) + \dots \quad (47) \end{aligned}$$

is obtained by considering all terms with an odd number of factors $\mathcal{A}^d(z, w)$. Then, it is easy to verify that

$$G_{ss}^{bc}(x, y) = \frac{1}{2} [G^{bc}(x, y) + G^{cb}(y, x)] \quad (48)$$

$$= G_e^{bc}(x, y) \quad (49)$$

$$G_{aa}^{bc}(x, y) = \frac{1}{2} [G^{bc}(x, y) - G^{cb}(y, x)] \quad (50)$$

$$= G_o^{bc}(x, y), \quad (51)$$

[where we considered again the decomposition (41)], and that [107]

$$G_o^{bc}(x, y) = f^{bde} \mathcal{S}^{-1}(x, z) \mathcal{A}^e(z, w) G_e^{dc}(w, y) \quad (52)$$

$$\begin{aligned} G_e^{bc}(x, y) &= \delta^{bc} \mathcal{S}^{-1}(x, y) \\ &\quad + f^{bdh} \mathcal{S}^{-1}(x, z) \mathcal{A}^h(z, w) G_o^{dc}(w, y). \quad (53) \end{aligned}$$

Thus, for the ghost propagator $G(x, y)$ — defined on the lattice as $\text{Tr} \mathcal{M}_U^{-1} / (N_c^2 - 1)$ — we obtain

$$G(x, y) = \frac{\delta^{bc}}{N_c^2 - 1} G^{bc}(x, y) = \frac{\delta^{bc}}{N_c^2 - 1} G_e^{bc}(x, y), \quad (54)$$

while for ghost condensation (in the Overhauser channel) we consider [13] the quantity

$$\begin{aligned} \phi^b(x, y) &= \frac{1}{N_c} f^{bcd} G^{cd}(x, y) = \frac{1}{N_c} f^{bcd} G_o^{cd}(x, y) \quad (55) \\ &= \frac{f^{bcd} f^{ceh}}{N_c} \mathcal{S}^{-1}(x, z) \mathcal{A}^h(z, w) G_e^{ed}(w, y). \quad (56) \end{aligned}$$

Also, in momentum space we have

$$G(p) = \frac{\delta^{bc}}{V(N_c^2 - 1)} \sum_{xy} G_e^{bc}(x, y) e^{-ip(x-y)} \quad (57)$$

$$= \frac{\delta^{bc}}{V(N_c^2 - 1)} \sum_{xy} G_e^{bc}(x, y) \cos[p(x-y)], \quad (58)$$

where in the last equation we used the symmetry of $G_e^{bc}(x, y)$ with respect to the space-time coordinates x and y . At the same time, we find

$$\phi^b(p) = \frac{f^{bcd}}{V N_c} \sum_{xy} G_o^{cd}(x, y) e^{-ip(x-y)} \quad (59)$$

$$= -i \frac{f^{bcd}}{V N_c} \sum_{xy} G_o^{cd}(x, y) \sin[p(x-y)]. \quad (60)$$

Considering the result (56) we can also write

$$\phi^b(p) = \frac{f^{bcd} f^{ceh}}{N_c} \langle p | \mathcal{S}^{-1} | q \rangle \langle q | \mathcal{A}^h | k \rangle \langle k | G_e^{ed} | p \rangle, \quad (61)$$

where we used Dirac notation and sums over q and k are understood. In order to simplify our analysis we can work in the continuum. Then, the matrix $\mathcal{S}(x, y)$ is given by $-\partial_x^2 \delta(x-y)$ and $\mathcal{A}^h = 2 g_0 A_\mu^h \partial_\mu \delta(x-y)$ [see Eq. (33)]. Thus, we obtain

$$\langle p | \mathcal{S}^{-1} | q \rangle = \delta(p-q) p^{-2} \quad (62)$$

and

$$\langle q | \mathcal{A}^h | k \rangle = 2 i g_0 \tilde{A}_\mu^h(q-k) k_\mu. \quad (63)$$

Here $\tilde{A}_\mu^h(p)$ is the Fourier-transformed gluon field defined (in the continuum and in d dimensions) as

$$\tilde{A}_\mu^h(p) = \frac{1}{(2\pi)^d} \sum_x A_\mu^h(x) e^{-i p x}. \quad (64)$$

Using the above results and $\langle k | G_e^{ed} | p \rangle = G_e^{ed}(k, p)$ we find

$$\phi^b(p) = \frac{f^{bcd} f^{ceh}}{N_c} \frac{2 i g_0 k_\mu \tilde{A}_\mu^h(p-k) G_e^{ed}(k, p)}{p^2}, \quad (65)$$

where a sum over the momenta k is understood. Note that, if $G_e^{bc}(k, p)$ is diagonal in color space, i.e. if

$$G_e^{bc}(k, p) = \delta^{bc} G_e^{bb}(k, p), \quad (66)$$

Eq. (65) simplifies to

$$\begin{aligned} \phi^b(p) &= \frac{f^{bce} f^{ceh}}{N_c} \frac{2 i g_0 k_\mu \tilde{A}_\mu^h(p-k) G_e^{dd}(k, p)}{p^2} \quad (67) \\ &= \frac{2 i g_0 k_\mu \tilde{A}_\mu^b(p-k) G_e^{dd}(k, p)}{p^2}, \quad (68) \end{aligned}$$

where we used $f^{bce} f^{ceh} = N_c \delta^{bh}$.

Finally, from Eq. (53) one obtains that the off-diagonal *symmetric* components of the ghost propagator $G_e^{bc}(x, y)$ are proportional to the off-diagonal *anti-symmetric* components $G_o^{bc}(x, y)$, being

$$G_e^{bc}(x, y) = f^{bdh} \mathcal{S}^{-1}(x, z) \mathcal{A}^h(z, w) G_o^{dc}(w, y). \quad (69)$$

In analogy with Eq. (65), one finds (in momentum space and in the continuum)

$$G_e^{bc}(p) = f^{bdh} \frac{2 i g_0 k_\mu \tilde{A}_\mu^h(p-k) G_o^{dc}(k, p)}{p^2}. \quad (70)$$

At the same time, for the ghost propagator, we can write [using Eqs. (53) and (54)]

$$\begin{aligned} G(x, y) &= \mathcal{S}^{-1}(x, y) \\ &+ \frac{f^{cdh}}{N_c^2 - 1} \mathcal{S}^{-1}(x, z) \mathcal{A}^h(z, w) G_o^{dc}(w, y) \quad (71) \\ &= \mathcal{S}^{-1}(x, z) \left[\delta(z - y) \right. \\ &\quad \left. - \mathcal{A}^h(z, w) \frac{N_c}{N_c^2 - 1} \phi^h(w, y) \right]. \quad (72) \end{aligned}$$

Note that the above expression can be used to derive Eq. (27) of Ref. [59].

A. Global gauge transformation

Let us note that the term $\mathcal{A}^b(x, y)$ is linear in the gluon field $A_\mu^d(x)$ [see Eqs. (32) and (42)]. Therefore, if we apply the transformation

$$A_\mu^d(x) \rightarrow -A_\mu^d(x), \quad (73)$$

then the ghost propagator $G(x, y)$ does not change, while the quantity $\phi^b(x, y)$ gets multiplied by -1 . Moreover, as we have seen in the previous section, when $G_e^{bc}(x, y)$ is diagonal in color space, the quantity $\phi^b(p)$ (in the continuum) is proportional to the Fourier-transformed gluon field \tilde{A}_μ^b [see Eq. (68)].

Let us also stress that, for a given color index b , one can always find a global gauge transformation that changes the sign of $\tilde{A}_\mu^b(q)$. For example, in the $SU(2)$ case and with $b = 3$ this can be achieved by using the x -independent gauge transformation

$$g = i \sigma^1 g_1 + i \sigma^2 g_2 \quad (74)$$

with $g_1^2 + g_2^2 = 1$. Indeed, if $g = i \sum_b \sigma^b g_b$, then the quantity

$$\frac{1}{V} g \left[\sum_x U_\mu(x) e^{-i \tilde{q} x} \right] g^\dagger \quad (75)$$

$$= g \left[\tilde{U}_\mu^0(\hat{q}) \mathbb{1} + i \sigma^c \tilde{A}_\mu^c(\hat{q}) \right] g^\dagger \quad (76)$$

becomes

$$\tilde{U}_\mu^0(\hat{q}) \mathbb{1} + 2 i \tilde{A}_\mu^c(\hat{q}) g_c \sigma^b g_b - i \tilde{A}_\mu^c(\hat{q}) \sigma^c. \quad (77)$$

Thus, if $g_3 = 0$ one immediately finds that the sign of $\tilde{A}_\mu^3(\hat{q})$ has changed (for any value of the index μ and any momentum \hat{q}). Here we considered the decomposition (10) for the $SU(2)$ link variables $U_\mu(x)$ and the definitions

$$\tilde{U}_\mu^0(\hat{q}) = \frac{1}{V} \sum_x U_\mu^0(x) e^{-i \tilde{q} x} \quad (78)$$

$$\tilde{A}_\mu^b(\hat{q}) = \frac{1}{V} \sum_x A_\mu^b(x) e^{-i \tilde{q} x}. \quad (79)$$

In the general $SU(N_c)$ case (with $N_c \geq 2$), changing the sign of $\tilde{A}_\mu^b(\hat{q})$ gives the relation

$$\begin{aligned} \text{Im Tr} \left[g \sum_x U_\mu(x) e^{-i \tilde{q} x} g^\dagger \lambda^b \right] \\ = -\text{Im Tr} \left[\sum_x U_\mu(x) e^{-i \tilde{q} x} \lambda^b \right] \quad (80) \end{aligned}$$

or

$$\text{Im Tr} \left[\sum_x U_\mu(x) e^{-i \tilde{q} x} (g^\dagger \lambda^b g + \lambda^b) \right] = 0, \quad (81)$$

where g is a global gauge transformation and we used Eq. (14). Then, a sufficient condition to satisfy the above equation is given by

$$g^\dagger \lambda^b g + \lambda^b = 0, \quad (82)$$

Lattice Volume V	8^4	12^4	16^4	20^4	24^4
No. of Configurations	1000	700	400	300	100

TABLE I: Lattice volumes and total number of configurations considered.

β	2.2	2.3	2.4
σa^2	0.220(9)	0.136(2)	0.071(1)
a (GeV $^{-1}$)	1.07(2)	0.838(6)	0.606(4)

TABLE II: Lattice string tension and lattice spacing (in physical units) for each lattice coupling β considered in our simulations. We used $\sqrt{\sigma} = 0.44$ GeV as physical input.

implying

$$\{\lambda^b, g\} = 0. \quad (83)$$

Clearly, in the $SU(2)$ case with $b = 3$ this yields $g = i\sigma^b g_b$ and $g_3 = 0$. Note that the choice

$$g = i \frac{\sigma_1 \tilde{A}_\mu^1(\hat{q}) + \sigma_2 \tilde{A}_\mu^2(\hat{q})}{\sqrt{[\tilde{A}_\mu^1(\hat{q})]^2 + [\tilde{A}_\mu^2(\hat{q})]^2}} \quad (84)$$

does not to change the values of $\tilde{A}_\mu^1(\hat{q})$ and $\tilde{A}_\mu^2(\hat{q})$. Of course, any other choice for g_1 and g_2 (with $g_3 = 0$) would still change the sign of $\tilde{A}_\mu^3(\hat{q})$ but would modify the values of the other two color components of $\tilde{A}_\mu(\hat{q})$. In any case, a global gauge transformation does not change the value of $\tilde{U}_\mu^0(\hat{q})$ in Eq. (76) above, implying that the quantity $\sum_c [\tilde{A}_\mu^c(\hat{q})]^2$ is also left unchanged.

IV. LATTICE SIMULATIONS

We performed numerical simulations of pure $SU(2)$ Yang-Mills theory in Landau gauge considering the standard Wilson action in four dimensions [108]. To thermalize the field configurations we used the heat-bath algorithm accelerated by *hybrid overrelaxation* (for details see [71, 72, 73]). In Table I we show the lattice volumes used in the simulations and the corresponding numbers of configurations. For *each* volume we have considered three values of the lattice coupling: $\beta = 2.2, 2.3$ and 2.4 . The corresponding string tensions in lattice units [72, 74] are given in Table II. In the same table we also report the lattice spacing in physical units for each coupling β , using $\sqrt{\sigma} = 0.44$ GeV as physical input.

The minimal (lattice) Landau gauge is implemented using the stochastic overrelaxation algorithm [75, 76, 77]. We stop the gauge fixing when the quantity

$$(\nabla \cdot A)^2 = \frac{1}{V} \sum_x \sum_b [(\nabla \cdot A^b)(x)]^2 \quad (85)$$

is smaller than 10^{-13} . In order to check for possible Gribov-copy effects we have also done (for each thermalized configuration) a second gauge fixing using the so-called smearing method [78]. (See again [73] for details.)

Ghost condensation in the Overhauser channel is studied by evaluating (here $N_c = 2$)

$$\langle i\phi^b(\hat{p}) \rangle = \frac{\epsilon^{bcd}}{2V} \sum_{xy} \langle G^{cd}(x,y) \rangle \sin[\hat{p}(x-y)] \quad (86)$$

as a function of the lattice momentum \hat{p} , with $G^{cd}(x,y)$ defined in Eq. (39). For the inversion of the lattice Faddeev-Popov matrix \mathcal{M}_U we employ a conjugate gradient (CG) method with even/odd preconditioning. Since this inversion has to be performed in the sub-space orthogonal to the constant modes — corresponding to null eigenvalues of \mathcal{M}_U — we verify at each CG iteration if the solution has indeed a zero constant component.

We also consider the average of the absolute value of $\phi^b(\hat{p})$. Using the continuum result (68), we should obtain

$$\langle |\phi^b(p)| \rangle \approx \frac{6g_0 k_\mu \langle |\tilde{A}_\mu^b(p-k)| G_e^{dd}(k,p) \rangle}{p^2}. \quad (87)$$

This result is valid when the propagator $G_e^{ed}(k,p)$ is diagonal in color space, but it should give a good approximation for $\langle |\phi^b(p)| \rangle$ also if $G_e^{ed}(k,p)$ is strongly diagonally-dominant. Let us recall that a matrix M_{ij} is strongly (or strictly) diagonally-dominant [109] if $M_{ii} > \sum_{j \neq i} M_{ij}$ for any i . We will verify this hypothesis in Section V.

Notice that a generic lattice momentum \hat{p} has components (in lattice units) $\hat{p}_\mu = 2 \sin(\pi \tilde{p}_\mu a/L_\mu)$ and that the magnitude (squared) of the lattice momentum is given by $\hat{p}^2 = \sum_\mu \hat{p}_\mu^2$. Here $L_\mu = a N_\mu$ is the physical size of the lattice in the μ direction, the quantity \tilde{p}_μ takes values $\lfloor \frac{-N_\mu}{2} \rfloor + 1, \dots, \lfloor \frac{N_\mu}{2} \rfloor$ and N_μ is the number of lattice points in the μ direction. Thus, if we keep the physical size L_μ constant and indicate with p_μ the momentum components in the continuum, we find that the lattice components $\hat{p}_\mu = a p_\mu$ take values in the interval $(-\pi, \pi]$ when $a \rightarrow 0$.

In order to analyze the effects due to the breaking of rotational symmetry we consider two types of lattice momenta, i.e.

- asymmetric: $\hat{p}_1 = \hat{p}_2 = \hat{p}_3 = 0$ and $\hat{p}_4 \neq 0$,
- symmetric: $\hat{p}_1 = \hat{p}_2 = \hat{p}_3 = \hat{p}_4 \neq 0$.

For a symmetric lattice ($L_\mu = L$) we obtain

$$\hat{p} = \hat{p}_4 = 2 \sin\left(\frac{\pi \tilde{p} a}{L}\right) \quad (88)$$

in the first case and

$$\hat{p} = 2\hat{p}_\mu = 4 \sin\left(\frac{\pi \tilde{p} a}{L}\right) \quad (89)$$

in the second one. In both cases \tilde{p} takes the values $\frac{-N}{2} + 1, \dots, \frac{N}{2}$ since $N_\mu = N$ and N is always even.

Let us note that the term contributing to $|\phi^b(p)|$ when $k = p$ is given by

$$\frac{6 g_0 p_\mu \tilde{A}_\mu^b(0) G(p)}{p^2}. \quad (90)$$

Thus, if we neglect all the other terms appearing in Eq. (87) we find

$$\langle |\phi^b(p)| \rangle \propto \frac{p_\mu \langle \tilde{A}_\mu^b(0) | G(p) \rangle}{p^2} \quad (91)$$

$$\sim \frac{\langle G(p) \rangle}{p}. \quad (92)$$

Therefore, if the ghost propagator has the infrared behavior $\langle G(p) \rangle \sim 1/p^{2+2\kappa}$ we obtain (in this approximation)

$$\langle |\phi(p)| \rangle \sim \frac{1}{p^{3+2\kappa}}. \quad (93)$$

Clearly, for $\kappa = 0.5$ one gets $\langle G(p) \rangle \sim 1/p^3$ and $\langle |\phi(p)| \rangle \sim 1/p^4$. Let us recall that for the infrared exponent κ — in Landau gauge and in four dimensions — there are several analytic predictions (using Dyson-Schwinger equations) [80, 81, 82, 83, 84, 85, 86] with values in the interval [0.52, 1.00]. On the other hand, numerical studies have found a value of $\kappa \approx 0.25 - 0.35$ [60, 70, 87, 88, 89], both for the $SU(2)$ and $SU(3)$ cases. Recently, a value $\kappa = 0.22(5)$ has been obtained in the unquenched $SU(3)$ case [57]. Note that these numerical results for the infrared exponent κ represent a lower bound, since the value of κ increases when one is able to get data at smaller momenta using larger lattice volumes [57, 60, 87]. We investigate the infrared behavior of $\phi(p)$ from our data in Section V below. There we also comment on the approximation obtained by neglecting terms with $p \neq q$ in Eq. (87).

As already stressed in the Introduction, the dependence of $\phi(p)$ on $\tilde{A}(q)$ [see Eq. (65)] could explain the $1/L^2$ behavior observed for $\langle |\phi(p)| \rangle$. On the other hand, as mentioned before, this result does not imply that $\phi(p)$ is zero at infinite volume.

Finally, from Eq. (70) we obtain that the off-diagonal symmetric components of $\langle G_e^{bc}(p) \rangle$ should also be non-zero if the off-diagonal anti-symmetric components are non-vanishing. However, in this case — due to the factor $k_\mu \tilde{A}_\mu^h(p - k)/p^2$ — one should expect a more singular dependence on the inverse momentum $1/p$ and stronger finite-volume effects than those observed for the anti-symmetric components $\langle G_o^{bc}(p) \rangle$.

A. The ghost-gluon vertex

Following the notation in Refs. [73, 90], the ghost-gluon vertex function is given (on the lattice) by the relation

$$\Gamma_\mu^{bcd}(\hat{k}, \hat{p}) = \frac{V \langle \tilde{A}_\mu^b(\hat{k}) G^{cd}(\hat{p}) \rangle}{\langle D(\hat{k}) \rangle \langle G(\hat{s}) \rangle \langle G(\hat{p}) \rangle}, \quad (94)$$

where $\tilde{s} = \tilde{k} + \tilde{p}$, $\langle D(\hat{k}) \rangle$ is the lattice gluon propagator and $\tilde{A}_\mu^b(\hat{k})$ is defined in Eq. (79). At tree-level (on the lattice) one has [91]

$$\Gamma_\mu^{bcd}(\hat{k}, \hat{p}) = i g_0 f^{bcd} \hat{p}_\mu \cos\left(\frac{\pi \tilde{s}_\mu a}{L_\mu}\right). \quad (95)$$

Thus, we can write

$$\Gamma_\mu^{bcd}(\hat{k}, \hat{p}) = i g_0 f^{bcd} \hat{p}_\mu \cos\left(\frac{\pi \tilde{s}_\mu a}{L_\mu}\right) \Gamma(\hat{k}, \hat{p}) \quad (96)$$

and at the asymmetric point, with zero momentum for the gluon ($\hat{k} = 0$), we find [73]

$$\begin{aligned} \Xi(\hat{p}) &= \frac{-i}{g_0 N_c (N_c^2 - 1)} \frac{1}{\hat{p}^2} \sum_\mu \frac{\hat{p}_\mu}{\cos\left(\frac{\pi \tilde{p}_\mu a}{L_\mu}\right)} \\ &\quad \times \frac{V f^{bcd} \langle \tilde{A}_\mu^b(0) G^{cd}(\hat{p}) \rangle}{\langle D(0) \rangle \langle G(\hat{p}) \rangle^2}, \end{aligned} \quad (97)$$

where we set $\Xi(\hat{p}) = \Gamma(0, \hat{p})$. Note that the combination $f^{bcd} G^{cd}(\hat{p})/N_c$ is the same that appears in the definition of $\phi^b(\hat{p})$. This gives

$$\begin{aligned} \Xi(\hat{p}) &= \frac{-i}{g_0 (N_c^2 - 1)} \frac{1}{\hat{p}^2} \sum_\mu \frac{\hat{p}_\mu}{\cos\left(\frac{\pi \tilde{p}_\mu a}{L_\mu}\right)} \\ &\quad \times \frac{V \langle \tilde{A}_\mu^b(0) \phi^b(\hat{p}) \rangle}{\langle D(0) \rangle \langle G(\hat{p}) \rangle^2}. \end{aligned} \quad (98)$$

On the other hand, since in the above equation the quantity $\phi^b(\hat{p})$ is multiplied by $\tilde{A}_\mu^b(0)$, one gets that the scalar function $\Xi(\hat{p})$ does not change sign under the transformation (73). This explains why there is no sign problem [73, 90] when evaluating the ghost-gluon-vertex renormalization function $\tilde{Z}_1^{-1}(\hat{p}) = \Xi(\hat{p})$.

Let us also note that the factor $\cos(\pi \tilde{p}_\mu a/L_\mu)$, which appears in the tree-level result (95) and in the denominator of Eq. (98), is a discretization effect that goes to 1 in the formal continuum limit $a \rightarrow 0$. Due to the relation between $\Xi(\hat{p})$ and $\phi^b(\hat{p})$ [see Eq. (98)], it is likely that similar discretization effects come up also in the present work. This will be verified in the next section.

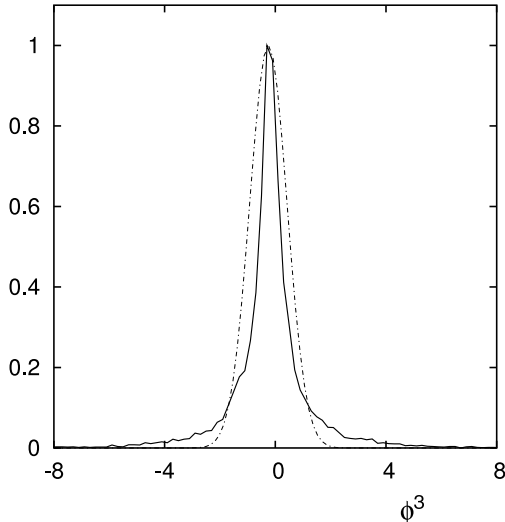


FIG. 2: Histogram (solid curve) of $\phi^3(\hat{p})$ for the lattice volume 8^4 with $\beta = 2.4$ and $\tilde{p} = (0, 0, 0, 1)$, using 10,000 configurations. For comparison we also plot a Gaussian distribution (dot-dashed line) with the same mean value and the same standard deviation.

V. RESULTS

We start our analysis of the data by considering the two Fourier-transformed quantities

$$G_e^{bd}(\hat{p}) = \frac{1}{V} \sum_{x,y} G^{bd}(x,y) \cos[\tilde{p}(x-y)] \quad (99)$$

$$G_o^{bd}(\hat{p}) = \frac{1}{V} \sum_{x,y} G^{bd}(x,y) \sin[\tilde{p}(x-y)]. \quad (100)$$

As explained in Section III, we expect $G_e^{bd}(\hat{p})$ [respectively $G_o^{bd}(\hat{p})$] to be symmetric (respectively anti-symmetric) in the color indices b and d . We have verified this by evaluating, for *each* configuration and for *each* momentum \hat{p} , the quantities

$$\left| \frac{G_e^{bd}(\hat{p}) - G_e^{db}(\hat{p})}{[G_e^{bd}(\hat{p}) + G_e^{db}(\hat{p})]/2} \right| \quad (101)$$

$$\left| \frac{G_o^{bd}(\hat{p}) + G_o^{db}(\hat{p})}{[G_o^{bd}(\hat{p}) - G_o^{db}(\hat{p})]/2} \right|, \quad (102)$$

which should both be zero. We find that these two quantities are usually very small, being respectively of the order of 10^{-3} and 10^{-6} . At the same time, we checked the hypothesis of strong diagonal-dominance for the symmetric components $G_e^{bd}(\hat{p})$. We obtain that the relation

$$|G_e^{bb}(\hat{p})| > \left| \sum_{d \neq b} G_e^{bd}(\hat{p}) \right| \quad (103)$$

is satisfied for *almost all* momenta \hat{p} and configurations (except for 14 cases out of 280800). This is expected since, due to the global color symmetry and for a zero ghost condensate v , one should have $\langle G_e^{ed}(\hat{p}) \rangle \propto \delta^{ed}$, after averaging over the gauge-fixed Monte Carlo configurations. Thus, it seems reasonable to assume that $G_e^{ed}(\hat{p})$ is strongly diagonally-dominant already for each configuration. This should also happen if the ghost condensate v is nonzero and small. We also considered the propagator $G_e^{bd}(\hat{k}, \hat{p})$ with $\hat{k} \neq \hat{p}$ for the lattice volume 8^4 and $\beta = 2.4$ with \tilde{k} given by $(0, 0, 0, 1)$ in the asymmetric case and by $(1, 1, 1, 1)$ in the symmetric one. In this case we find that the relation

$$|G_e^{bb}(\hat{k}, \hat{p})| > \left| \sum_{d \neq b} G_e^{bd}(\hat{k}, \hat{p}) \right| \quad (104)$$

is satisfied in about 75% of the cases.

We then evaluated the average of [see Eq. (86)]

$$i\phi^b(\hat{p}) = \frac{i\epsilon^{bcd}}{2} G^{cd}(\hat{p}) = \frac{\epsilon^{bcd}}{2} G_o^{cd}(\hat{p}) \quad (105)$$

for $b = 1, 2, 3$. We find that this quantity is consistent with zero, within one standard deviation [110]. Indeed, the statistical fluctuations are always very large, being larger than the central value for more than 60% of the data points and larger than 1/3 of the central value for all our data. On the contrary, when considering the absolute value of $\phi^b(\hat{p})$ we find a relatively small error,

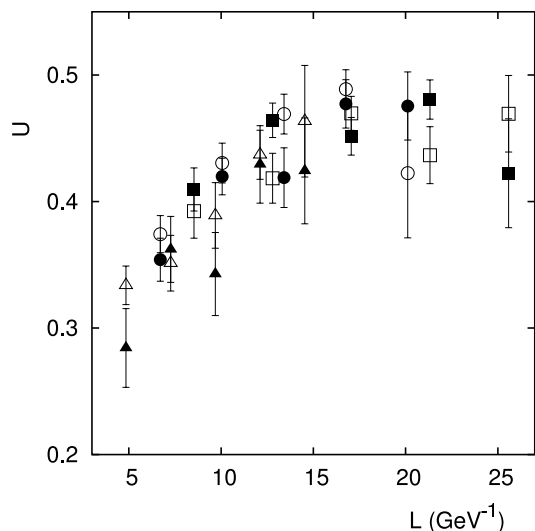


FIG. 3: Results for the Binder cumulant U [defined in Eq. (1)] for the quantity $\phi^b(\hat{p})$ as a function of the lattice side L (in GeV^{-1}) for all lattice volumes V , couplings β and momenta with $\tilde{p} = N/4$. We show the data corresponding to asymmetric momenta [for $\beta = 2.2$ (\square), $\beta = 2.3$ (\circ) and $\beta = 2.4$ (\triangle)] and to symmetric momenta (with the corresponding filled symbols for each β). Errors have been estimated using the bootstrap method with 10,000 samples.

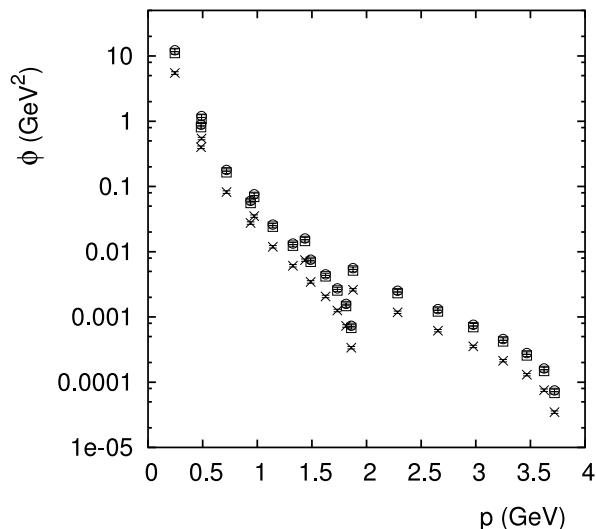


FIG. 4: Results for ϕ_a (\times), ϕ_m (\square) and ϕ_r (\circ) [defined in Eqs. (106)–(108)] as a function of the momentum p for lattice volume $V = 24^4$ and $\beta = 2.2$. We show the data corresponding to asymmetric and to symmetric momenta. Note the logarithmic scale on the y axis. Errors have been estimated using the bootstrap method with 10,000 samples.

of less than 10% of the central value in 99.7% of the cases. As discussed in the Introduction, this is a clear indication that the data for $\phi^b(\hat{p})$ do not correspond to a Gaussian distribution. We have verified this by comparing a histogram of the data with a Gaussian curve. Then, as for the $3d$ $O(4)$ nonlinear σ -model in the broken phase (see the Introduction), one finds (see Fig. 2) that the shape of the statistical distribution of the data is clearly not Gaussian. (However, notice that the shape of this non-Gaussian distribution is not the same as for the spin-model case.) We also find that working at constant physics, i.e. with approximately fixed lattice side L and momentum p (in physical units), the deviation from a Gaussian distribution increases when the lattice coupling β increases. Finally, we have looked at the Binder cumulant U [see Eq. (1)] for the order parameter $\phi^b(\hat{p})$. We find that U is clearly different from zero for all lattice sizes N , couplings β and momenta \hat{p} , and seems to converge to a value $U \approx 0.45$ as the lattice side L increases (see Fig. 3). This limiting value is essentially independent of the momentum p [111]. The data show good scaling for the three β values considered. As argued in the Introduction, the large fluctuations for $\phi^b(\hat{p})$ and the deviation from a Gaussian distribution could signal the spontaneous breaking of the global $SL(2, R)$ symmetry, implying a nonzero value for the ghost condensate v .

In order to plot the data for $|\phi^b(\hat{p})|$, we average over

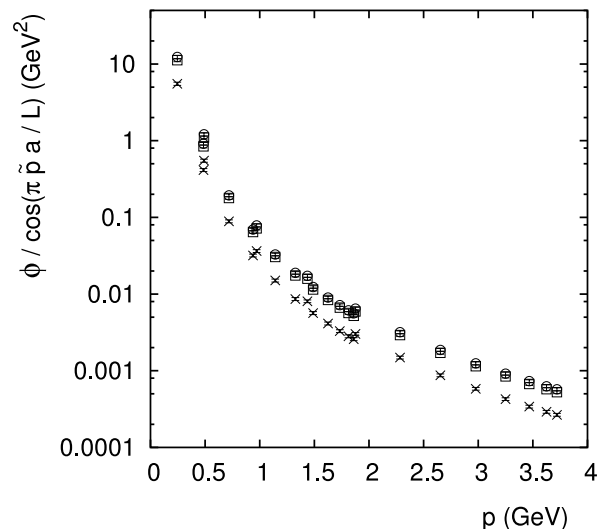


FIG. 5: Results for ϕ_a (\times), ϕ_m (\square) and ϕ_r (\circ) [defined in Eqs. (106)–(108)], divided by $\cos(\pi \tilde{p} a/L)$, as a function of the momentum p for lattice volume $V = 24^4$ and $\beta = 2.2$. We show the data corresponding to asymmetric and to symmetric momenta. Note the logarithmic scale on the y axis. Errors have been estimated using the bootstrap method with 10,000 samples.

the color index b considering the three quantities

$$\phi_a(\hat{p}) = \frac{1}{3} \sum_b \langle |\phi^b(\hat{p})| \rangle \quad (106)$$

$$\phi_m(\hat{p}) = \left\langle \sqrt{\frac{1}{3} \sum_b |\phi^b(\hat{p})|^2} \right\rangle \quad (107)$$

$$\phi_r(\hat{p}) = \sqrt{\left\langle \frac{1}{3} \sum_b |\phi^b(\hat{p})|^2 \right\rangle}, \quad (108)$$

i.e. we take (respectively) the average of the absolute value of the components of ϕ , the average of the absolute value of ϕ and the root mean square of ϕ . The results are shown in Fig. 4. In this figure the breaking of rotational symmetry is evident: the asymmetric and symmetric momenta clearly form two different curves. In particular, the three quantities decrease significantly at $p \approx 1.85$ GeV in the asymmetric case and at $p \approx 3.7$ GeV in the symmetric one.

The interpretation of the data is simpler (see Fig. 5) if one rescales $\phi^b(\hat{p})$ with the factor $\cos(\pi \tilde{p} a/L)$ that appears in the lattice formula for the ghost-gluon-vertex renormalization function [see Eq. (98) in Section IV A]. Moreover, as can be seen in Fig. 5, the effects due to the breaking of rotational symmetry are relatively small. Finally, we can multiply the data by L^2 to obtain the single curve shown in Fig. 6. Again, we find good scaling for the three β values considered. Let us recall that, for the gluon and ghost propagators in the $SU(2)$ case [72, 88],

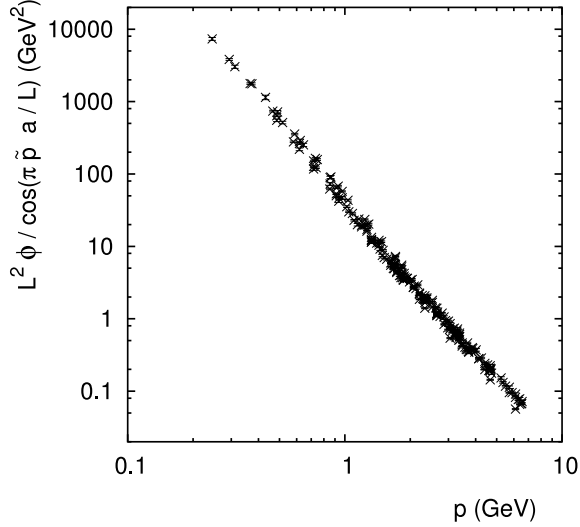


FIG. 6: Results for ϕ_m [defined in Eq. (107)], rescaled by $L^2 / \cos(\pi \tilde{p} a / L)$, as a function of the momentum p for all lattice volumes and β values considered. We show the data corresponding to asymmetric and to symmetric momenta. Note the logarithmic scale on the x and y axes. Errors have been estimated using the bootstrap method with 10,000 samples.

scaling has been observed in the range $\beta \in [2.15, 2.8]$. Note that, from our analysis in Section IV, we would expect (in the infrared limit) a behavior of the type $G(p)/p$ for the three quantities defined above, if the contribution proportional to $\tilde{A}(0)$ is dominant.

Let us recall that in the $SU(2)$ case the inverse Faddeev-Popov matrix — in the condensed Overhauser vacuum $\phi^b \propto \delta^{b3}$ — should be given (in momentum space) by [13]

$$G^{cd}(p) = \frac{p^2 \delta^{cd} + v \epsilon^{cd}}{p^4 + v^2}, \quad (109)$$

where ϵ^{cd} is the anti-symmetric tensor with $c, d = 1, 2$ and v is the ghost condensate, given (at one loop and for $N_c = 2$) by [13]

$$v = \left| \frac{\phi^3}{\rho_0} \right| = \left| \frac{\chi_{vac} (2N_f - 13)}{3} \right| \quad (110)$$

with $\chi_{vac} = 0.539 \Lambda_{\overline{MS}}^2$. Since in our case $N_f = 0$, we find

$$v \approx \frac{13}{3} 0.539 \Lambda_{\overline{MS}}^2 \approx 2.34 \Lambda_{\overline{MS}}^2. \quad (111)$$

Then, with $\Lambda_{\overline{MS}} \approx 250$ MeV, we obtain $v \approx 0.146$ GeV². A fit of the type

$$\frac{L^2}{\cos\left(\frac{\pi \tilde{p} a}{L}\right)} |\phi^b| = \frac{r}{p^z}, \quad (112)$$

Data considered	d.o.f.	r	z	$\chi^2/d.o.f.$
All data	208	37.3(7)	3.52(2)	6.54
$V = 24^4$ and $\beta = 2.2$	20	36(1)	3.65(5)	3.09
All data and $p < 2$ GeV	96	39.5(6)	3.79(3)	5.33
$V = 24^4$, $\beta = 2.2$ and $p < 2$ GeV	13	36(1)	3.80(5)	2.50
All data, $p < 2$ GeV, only symm. momenta	24	49(1)	3.82(5)	3.44
All data, $p < 2$ GeV, only asymm. momenta	70	37.7(4)	3.80(2)	3.35
$V = 24^4$, $\beta = 2.2$, only asymm. momenta	9	34.3(4)	3.80(2)	0.82

TABLE III: The parameters r and z obtained by fitting ϕ_m to the formula (112). We considered different sets of data. The fits have been done using `gnuplot`.

works quite well for our data, giving for the parameters r and z the results reported in Table III. Note that the exponent z increases systematically when one considers data at small momenta only, suggesting that z would approach 4 if one could really probe the infrared limit. We also tried a fit using the form $r/(p^z + v^2)$. The results obtained in this case are very similar to those reported in Table III, with v always consistent with zero within error bars. Furthermore, for the ghost propagator $G(p)$ we find that a fit to r/p^z yields z in the interval 2.33 – 2.46, depending on the set of data considered. Thus, the quantity $\phi(p)$ has a stronger infrared behavior than $G(p)/p$, which is obtained by neglecting terms with $p \neq q$ in Eq. (87).

By comparing the above fitting formula to the theoretical prediction (109), i.e. by considering (in the anti-symmetric case) the Ansatz [112]

$$G^{cd}(p) = \frac{r L^{-2} + v}{p^4 + v^2} \epsilon^{cd}, \quad (113)$$

we can state that

$$v \ll r L_{max}^{-2}, \quad v \ll p_{min}^2. \quad (114)$$

In our simulations we have $1/L_{max} \approx 0.039$ GeV and $p_{min} \approx 0.245$ GeV. Thus, using $r \approx 38$ (see Table III), we obtain our final estimate

$$v \ll 0.058 \text{ GeV}^2, \quad (115)$$

Note that, since $38 \approx (2\pi)^2$ and $p_{min} \approx 2\pi/L_{max}$, the two inequalities in (114) give practically the same estimate for the ghost condensate v . One can also try a fit of the data using the function $r/(p^z + v^2)$ with a fixed small value for v . Then, for $v \leq 0.025$ GeV² the values of $\chi^2/d.o.f.$ reported in Table III do not change significantly.

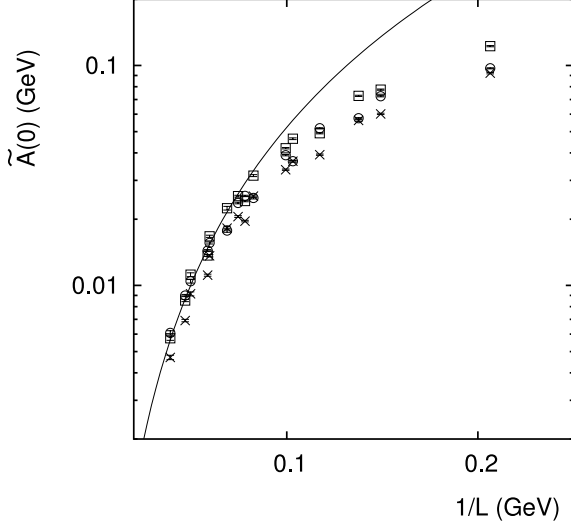


FIG. 7: Results for $\tilde{A}_a(0)$ (\times), $\tilde{A}_m(0)$ (\square) and $\tilde{A}_r(0)$ (\circ) [defined in Eqs. (116)–(118)] as a function of the inverse lattice side $1/L$ for all lattice volumes and β values considered. Errors have been estimated using the bootstrap method with 10,000 samples. We also report the fit of \tilde{A}_m to the function b/L^s with $b = 10(7)$ and $s = 2.4(2)$. When considering the data for $\tilde{A}_a(0)$, one finds for the exponent s the same value as above, while for $\tilde{A}_r(0)$ one gets $s = 2.0(1)$. In all cases, the fits have been done using `gnuplot` and we consider only the data corresponding to $1/L < 0.07$ GeV.

Now, we consider the dependence of $|\tilde{A}_\mu^b(q)|$ on the lattice side L in physical units. In analogy with Eqs. (106)–(108), we define the three quantities

$$\tilde{A}_a(q) = \frac{1}{12} \sum_b \sum_\mu \langle |\tilde{A}_\mu^b(q)| \rangle \quad (116)$$

$$\tilde{A}_m(q) = \left\langle \sqrt{\frac{1}{12} \sum_b |\tilde{A}_\mu^b(q)|^2} \right\rangle \quad (117)$$

$$\tilde{A}_r(q) = \sqrt{\left\langle \frac{1}{12} \sum_b |\tilde{A}_\mu^b(q)|^2 \right\rangle}. \quad (118)$$

As shown in Fig. 7, we find that the (absolute value of the) Fourier-transformed gluon field at zero momentum $\tilde{A}(0)$ goes to zero as L^{-s} with $s \approx 2$ for the three quantities defined above. Similar results can be obtained when $q \neq 0$ [113]. This is a confirmation that the finite-size effects observed for the quantity $\phi(p)$ are indeed induced by $\tilde{A}(q)$. We have also checked that the sign of $\phi^3(p)$ can be changed using the global gauge transformation reported in Eq. (74), i.e. by changing the sign of $\tilde{A}_\mu^3(q)$.

Finally, we study the off-diagonal symmetric components $G_e^{bc}(x,y)$ by considering the quantity $\psi^b(\hat{p}) = [G_e^{cd}(\hat{p}) + G_e^{dc}(\hat{p})]/2$, with $b \neq c, d$ and $b = 1, 2, 3$. Let us stress that, even though these components are

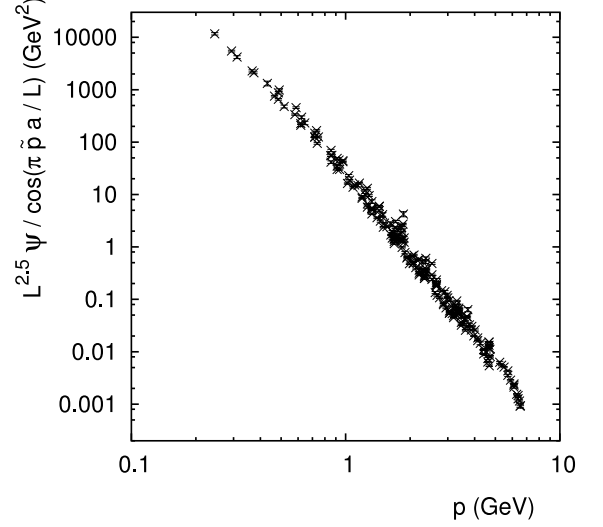


FIG. 8: Results for ψ_m [defined in Eq. (120)], rescaled by $L^{2.5}/\cos(\pi \tilde{p} a/L)$, as a function of the momentum p for all lattice volumes and β values considered. We show the data corresponding to asymmetric and to symmetric momenta. Note the logarithmic scale on the x and y axes. Errors have been estimated using the bootstrap method with 10,000 samples.

symmetric under the transformation (73), they are not necessarily positive [see Eq. (69)]. Thus, also in this case we should consider their absolute value. In analogy with the analysis reported above for $\phi^b(\hat{p})$, we can evaluate

$$\psi_a(\hat{p}) = \frac{1}{3} \sum_b \langle |\psi^b(\hat{p})| \rangle \quad (119)$$

$$\psi_m(\hat{p}) = \left\langle \sqrt{\frac{1}{3} \sum_b |\psi^b(\hat{p})|^2} \right\rangle \quad (120)$$

$$\psi_r(\hat{p}) = \sqrt{\left\langle \frac{1}{3} \sum_b |\psi^b(\hat{p})|^2 \right\rangle}. \quad (121)$$

We obtain that these quantities produce a single curve when rescaled by $L^{2.5}/\cos(\pi \tilde{p} a/L)$ (see Fig. 8). Note however that the rescaling does not work as well as for the ϕ 's. Also, the rescaled data can be reasonably well fitted using the fitting function s/p^z with $z \approx 5$. This is in agreement with the observation made before Section IV A and in partial agreement with the results reported in Ref. [60].

We have done the analysis reported above also for the gauge-fixed configurations obtained using the smearing method [78]. As for the ghost-gluon vertex [73, 90], we find that the contribution of Gribov-copy effects (if present) is always zero within error bars. In particular, the exponent z obtained when fitting the functions $\phi(p)$ is close to 4 at small momenta also when using the smearing method.

VI. CONCLUSIONS

We study numerically the off-diagonal components of the momentum-space ghost propagator $G^{cd}(p)$ for $SU(2)$ lattice gauge theory in minimal Landau gauge. We see clear signs of spontaneous breaking of a global symmetry, using the quantity $\phi^b(p) = \epsilon^{bcd}G^{cd}(p)/2$ as order parameter. As in the case of continuous-spin models in the ordered phase, we find indication of spontaneous symmetry breaking from two (related) observations: 1) by comparing the statistical fluctuations for the quantities $\phi^b(p)$ and $|\phi^b(p)|$; 2) from the non-Gaussian shape of the statistical distribution of $\phi^b(p)$, which can be observed by considering a histogram of the data or by evaluating the so-called Binder cumulant. Since, in Landau gauge, the vacuum expectation value of the quantity $\phi^b(p)$ should be proportional (in the so-called Overhauser channel) to the ghost condensate v [13], it seems reasonable to conclude that the broken symmetry is the $SL(2, R)$ symmetry, which is related to ghost condensation [6, 42]. Let us note that, from our data, the Binder cumulant U seems to be approximately null at small lattice volume and to converge to a value $U \approx 0.45$ for physical lattice side $L \gtrsim 15 \text{ GeV}^{-1} \approx 3 \text{ fm}$, corresponding to a mass scale of less than 100 MeV.

As stressed in the Introduction, we have shown that the dependence of $\phi^b(p)$ on $\tilde{A}_\mu^d(q)$ [see Eq. (87)] can explain the $1/L^2$ behavior observed for $\langle |\phi(p)| \rangle$. We have also shown that $\phi^b(p)$ has discretization effects similar to those obtained for the ghost-gluon vertex [73, 90]. Then, using the rescaled quantity $|L^2 \phi^b(p)/\cos(\pi\tilde{p}a/L)|$, we find a behavior p^{-z} with $z \approx 4$, in agreement with analytic predictions [13]. It is important to note that this result is not obtained just by considering the approximation $\phi(p) \approx G(p)/p$ [see Eq. (92)], since our data for the ghost propagator $G(p)$ have an infrared behavior given by $1/p^{2.4}$. We therefore view the similar momentum dependence obtained numerically and analytically for $\phi^b(p)$ as

a further indication of ghost condensation. On the other hand, from our fits we find that the ghost condensate v is consistent with zero within error bars, i.e. the quantity $|L^2 \phi^b(p)/\cos(\pi\tilde{p}a/L)|$ does not approach a finite limit at small momenta, at least for $p \geq 0.245 \text{ GeV}$. Using the Ansatz (113) we obtain for the ghost condensate the upper bound $v \ll 0.058 \text{ GeV}^2$. More precisely, our data rule out values of v greater than $0.058 \text{ GeV}^2 \approx (240 \text{ MeV})^2$ but would still be consistent with a ghost condensate $v \lesssim 0.025 \text{ GeV}^2 \approx (160 \text{ MeV})^2$. As said in the Introduction, in analytic studies [10, 13, 23, 92] one finds that the ghost condensate induces a tachyonic gluon mass proportional to \sqrt{v} , which modifies the dynamic gluon mass related to the gauge condensate $\langle A_\mu^b A_\mu^b \rangle$. Thus, one should expect a relatively small ghost condensate v in order to obtain a global (non-tachyonic) gluon mass. Let us recall that a dynamic gluon mass of the order of a few hundred MeV has been considered in several phenomenological studies [93, 94, 95, 96, 97]. A similar mass scale was also obtained in numerical studies of the gluon propagator in Landau gauge [98, 99, 100, 101].

We plan to extend our simulations to larger lattice volumes, up to 48^4 , which would allow us to detect a ghost condensate as small as $v \approx 0.01 \text{ GeV}^2 = (100 \text{ MeV})^2$.

ACKNOWLEDGMENTS

We thank S. P. Sorella and R. F. Sobreiro for many helpful discussions and the IF-UERJ in Rio de Janeiro for the kind hospitality during our visits there. We also thank S. Furui, H. Nakajima, M. Schaden and D. Zwanziger for useful comments and suggestions on the manuscript and D. Dudal for sending us Ref. [23] before submittal to arXiv.org. This research was supported by FAPESP (Projects No. 00/05047-5 and 03/00928-1). Partial support from CNPq is also acknowledged (AC, TM).

-
- [1] E. V. Shuryak, *The QCD vacuum, hadrons and the superdense matter*, World Scientific (1988, Singapore).
 - [2] M. A. Shifman, A. I. Vainshtein and V. I. Zakharov, Nucl. Phys. B **147**, 385 (1979).
 - [3] M. A. Shifman, A. I. Vainshtein and V. I. Zakharov, Nucl. Phys. B **147**, 448 (1979).
 - [4] F. V. Gubarev, L. Stodolsky and V. I. Zakharov, Phys. Rev. Lett. **86**, 2220 (2001).
 - [5] F. V. Gubarev and V. I. Zakharov, Phys. Lett. B **501**, 28 (2001).
 - [6] D. Dudal *et al.*, JHEP **0212**, 008 (2002).
 - [7] V. E. R. Lemes, M. S. Sarandy and S. P. Sorella, J. Phys. A **36**, 7211 (2003).
 - [8] V. E. R. Lemes *et al.*, Mod. Phys. Lett. A **18**, 711 (2003).
 - [9] V. E. R. Lemes, M. S. Sarandy and S. P. Sorella, Annals Phys. **308**, 1 (2003).
 - [10] D. Dudal and H. Verschelde, J. Phys. A **36**, 8507 (2003).
 - [11] D. Dudal, H. Verschelde and S. P. Sorella, Phys. Lett. B **555**, 126 (2003).
 - [12] D. Dudal *et al.*, Annals Phys. **308**, 62 (2003).
 - [13] D. Dudal *et al.*, JHEP **0306**, 003 (2003).
 - [14] D. Dudal *et al.*, Phys. Lett. B **569**, 57 (2003).
 - [15] D. Dudal *et al.*, Phys. Lett. B **574**, 325 (2003).
 - [16] D. Dudal *et al.*, JHEP **0401**, 044 (2004).
 - [17] R. F. Sobreiro, S. P. Sorella, D. Dudal and H. Verschelde, Phys. Lett. B **590**, 265 (2004).
 - [18] D. Dudal *et al.*, Phys. Rev. D **70**, 114038 (2004).
 - [19] D. Dudal *et al.*, Annals Phys. **317**, 203 (2005).
 - [20] D. Dudal, J. A. Gracey, V. E. R. Lemes, M. S. Sarandy, R. F. Sobreiro, S. P. Sorella and H. Verschelde, hep-th/0501227.
 - [21] D. Dudal, R. F. Sobreiro, S. P. Sorella and H. Verschelde, Phys. Rev. D **72**, 014016 (2005).

- [22] D. Dudal *et al.*, JHEP **0507**, 059 (2005).
- [23] M. A. L. Capri *et al.*, hep-th/0508216.
- [24] A. A. Slavnov, Theor. Math. Phys. **143**, 489 (2005) [Teor. Mat. Fiz. **143**, 3 (2005)].
- [25] A. A. Slavnov, Phys. Lett. B **608**, 171 (2005).
- [26] D. V. Bykov and A. A. Slavnov, hep-th/0505089.
- [27] K. I. Kondo and T. Shinohara, Phys. Lett. B **491**, 263 (2000).
- [28] K. I. Kondo, hep-th/0103141.
- [29] K. I. Kondo, Phys. Lett. B **514**, 335 (2001).
- [30] K. I. Kondo, T. Murakami, T. Shinohara and T. Imai, Phys. Rev. D **65**, 085034 (2002).
- [31] K. I. Kondo, Phys. Lett. B **560**, 44 (2003).
- [32] K. I. Kondo, Phys. Lett. B **572**, 210 (2003).
- [33] K. I. Kondo, hep-th/0307270.
- [34] K. I. Kondo, Phys. Lett. B **619**, 377 (2005).
- [35] G. 't Hooft, Nucl. Phys. B **190**, 455 (1981).
- [36] T. Suzuki, Nucl. Phys. Proc. Suppl. **30**, 176 (1993).
- [37] M. N. Chernodub, F. V. Gubarev, M. I. Polikarpov and A. I. Veselov, Prog. Theor. Phys. Suppl. **131**, 309 (1998).
- [38] D. Zwanziger, Nucl. Phys. B **412**, 657 (1994).
- [39] M. Schaden, hep-th/9909011.
- [40] M. Schaden, hep-th/0003030, in the Proceedings of the 5th Workshop on *Quantum chromodynamics*, Villefranche-sur-Mer, France, 2000, edited by H. M. Fried *et al.* (World Scientific, Singapore, 2000) 46.
- [41] M. Schaden, hep-th/0108034, in the Proceedings of 4th International Conference on *Quark confinement and the hadron spectrum*, Wien, Austria, 2000, edited by W. Lucha and K. M. Maung (World Scientific, Singapore, 2001) 258.
- [42] R. Alkofer and L. von Smekal, Phys. Rept. **353**, 281 (2001).
- [43] J. Bardeen, L. N. Cooper and J. R. Schrieffer, Phys. Rev. **106**, 162 (1957).
- [44] J. Bardeen, L. N. Cooper and J. R. Schrieffer, Phys. Rev. **108**, 1175 (1957).
- [45] A. W. Overhauser, Advances in Physics **27**, 343 (1978).
- [46] Z. F. Ezawa and A. Iwazaki, Phys. Rev. D **25**, 2681 (1982).
- [47] T. Suzuki, Prog. Theor. Phys. **81**, 752 (1989).
- [48] K. Amemiya and H. Suganuma, Phys. Rev. D **60**, 114509 (1999).
- [49] V. G. Bornyakov, M. N. Chernodub, F. V. Gubarev, S. M. Morozov and M. I. Polikarpov, Phys. Lett. B **559**, 214 (2003).
- [50] Y. Nambu, Phys. Rev. D **10**, 4262 (1974).
- [51] S. Mandelstam, Phys. Rept. **23**, 245 (1976).
- [52] H. Suganuma and H. Ichie, Nucl. Phys. Proc. Suppl. **121**, 316 (2003).
- [53] P. Boucaud, A. Le Yaouanc, J. P. Leroy, J. Micheli, O. Pene and J. Rodriguez-Quintero, Phys. Rev. D **63**, 114003 (2001).
- [54] P. Boucaud *et al.*, Phys. Rev. D **66**, 034504 (2002).
- [55] P. Boucaud *et al.*, Phys. Rev. D **67**, 074027 (2003).
- [56] E. Ruiz Arriola, P. O. Bowman and W. Broniowski, Phys. Rev. D **70**, 097505 (2004).
- [57] S. Furui and H. Nakajima, arXiv:hep-lat/0503029.
- [58] P. Boucaud *et al.*, arXiv:hep-lat/0504017.
- [59] P. Boucaud *et al.*, arXiv:hep-ph/0507104.
- [60] S. Furui and H. Nakajima, Phys. Rev. D **69**, 074505 (2004).
- [61] K. Binder and D. W. Heermann, *Monte Carlo Simulation in Statistical Physics An Introduction*, Springer-Verlag (2002, Berlin).
- [62] O. G. Mouritsen, *Computer Studies of Phase Transitions and Critical Phenomena*, Springer-Verlag (1984, Berlin).
- [63] J. Engels and T. Mendes, Nucl. Phys. B **572**, 289 (2000).
- [64] D. Zwanziger, Phys. Lett. B **257**, 168 (1991).
- [65] A. Cucchieri, Nucl. Phys. B **521**, 365 (1998).
- [66] D. B. Leinweber, J. I. Skullerud, A. G. Williams and C. Parrinello [UKQCD Collaboration], Phys. Rev. D **60**, 094507 (1999) [Erratum-ibid. D **61**, 079901 (2000)].
- [67] P. Marenzoni, G. Martinelli, N. Stella and M. Testa, Phys. Lett. B **318**, 511 (1993).
- [68] P. Marenzoni, G. Martinelli and N. Stella, Nucl. Phys. B **455**, 339 (1995).
- [69] T. D. Bakeev, E. M. Ilgenfritz, V. K. Mitrjushkin and M. Mueller-Preussker, Phys. Rev. D **69**, 074507 (2004).
- [70] A. Sternbeck, E. M. Ilgenfritz, M. Mueller-Preussker and A. Schiller, Phys. Rev. D **72**, 014507 (2005).
- [71] A. Cucchieri, T. Mendes, G. Travieso and A. R. Taurines, hep-lat/0308005, in the Proceedings of the 15th Symposium on *Computer Architecture and High Performance Computing*, São Paulo SP, Brazil, 2003, edited by L.M. Sato *et al.* (IEEE Computer Society Press, Los Alamitos CA, 2003) 123.
- [72] J. C. R. Bloch, A. Cucchieri, K. Langfeld and T. Mendes, Nucl. Phys. B **687**, 76 (2004).
- [73] A. Cucchieri, T. Mendes and A. Mihara, JHEP **0412**, 012 (2004).
- [74] J. Fingberg, U. M. Heller and F. Karsch, Nucl. Phys. B **392**, 493 (1993).
- [75] A. Cucchieri and T. Mendes, Nucl. Phys. B **471**, 263 (1996).
- [76] A. Cucchieri and T. Mendes, Nucl. Phys. Proc. Suppl. **53**, 811 (1997).
- [77] A. Cucchieri and T. Mendes, Comput. Phys. Commun. **154**, 1 (2003).
- [78] J. E. Hetrick and P. de Forcrand, Nucl. Phys. Proc. Suppl. **63**, 838 (1998).
- [79] G. H. Golub and C. F. Van Loan, *Matrix computations*, The Johns Hopkins University Press (1989, second edition, Baltimore).
- [80] L. von Smekal, R. Alkofer and A. Hauck, Phys. Rev. Lett. **79**, 3591 (1997).
- [81] D. Atkinson and J. C. R. Bloch, Phys. Rev. D **58**, 094036 (1998).
- [82] D. Atkinson and J. C. Bloch, Mod. Phys. Lett. A **13**, 1055 (1998).
- [83] C. Lerche and L. von Smekal, Phys. Rev. D **65**, 125006 (2002).
- [84] C. S. Fischer, R. Alkofer and H. Reinhardt, Phys. Rev. D **65**, 094008 (2002).
- [85] D. Zwanziger, Phys. Rev. D **65**, 094039 (2002).
- [86] D. Zwanziger, Phys. Rev. D **67**, 105001 (2003).
- [87] A. Cucchieri, Nucl. Phys. B **508**, 353 (1997).
- [88] J. C. R. Bloch, A. Cucchieri, K. Langfeld and T. Mendes, Nucl. Phys. Proc. Suppl. **119**, 736 (2003).
- [89] S. Furui and H. Nakajima, Phys. Rev. D **70**, 094504 (2004).
- [90] A. Mihara, A. Cucchieri and T. Mendes, AIP Conf. Proc. **739**, 602 (2005).
- [91] H. Kawai, R. Nakayama and K. Seo, Nucl. Phys. B **189**, 40 (1981).
- [92] H. Sawayanagi, Phys. Rev. D **67**, 045002 (2003).

- [93] G. Parisi and R. Petronzio, Phys. Lett. B **94**, 51 (1980).
- [94] F. Halzen, G. I. Krein and A. A. Natale, Phys. Rev. D **47**, 295 (1993).
- [95] M. B. Gay Ducati, F. Halzen and A. A. Natale, Phys. Rev. D **48**, 2324 (1993).
- [96] J. H. Field, Phys. Rev. D **66**, 013013 (2002).
- [97] M. B. Gay Ducati and W. K. Sauter, arXiv:hep-ph/0501057.
- [98] A. Cucchieri, Phys. Rev. D **60**, 034508 (1999).
- [99] K. Langfeld, H. Reinhardt and J. Gattnar, Nucl. Phys. B **621**, 131 (2002).
- [100] A. Cucchieri, T. Mendes and A. R. Taurines, Phys. Rev. D **67**, 091502 (2003).
- [101] A. Cucchieri, T. Mendes and A. R. Taurines, Phys. Rev. D **71**, 051902 (2005).
- [102] See for example [61, Sections 2.3.3 and 2.3.4] and [62, Section 2.2.5].
- [103] Note that in Eq. (7) one should define the gluon field at the midpoint $A_\mu(x + e_\mu/2)$ (see for example [66]), but in our case we may ignore this subtlety.
- [104] Here we use the superscript (c) for quantities in the continuum only when necessary to avoid confusion between these and the corresponding lattice quantities.
- [105] Note that, in the $SU(N_c)$ case with $N_c \geq 3$, the second term on the r.h.s. of Eq. (8) is of order a^3 . Thus, the definition (9) can be used also for the $SU(3)$ case, corresponding to a different lattice discretization for the gluon field [67, 68].
- [106] This expansion can be used to evaluate numerically the ghost propagator (see for example [60]).
- [107] Note that Eq. (53) agrees with Eq. (20) in Ref. [59].
- [108] Simulations have been performed on several 866 MHz Pentium III and 1.7 GHz Pentium IV machines (with 256 MB RAM) at the IFSC-USP in São Carlos. The total CPU time was about 264 days on a Pentium III machine plus 61 days on a Pentium IV machine.
- [109] See for example Section 3.4.10 in Ref. [79].
- [110] All the errors have been evaluated using the bootstrap method with 10,000 samples. We checked that the errors calculated in this way are in agreement with the estimates obtained when considering one standard deviation.
- [111] We do not include in this analysis the momenta (asymmetric and symmetric) with $\tilde{p} = 1$ and with $\tilde{p} = N/2$, since they are often characterized by a Binder cumulant U with a very large statistical error.
- [112] Note that here we neglect the discretization effect related to the factor $\cos(\pi \tilde{p} a/L)$.
- [113] Of course, for a given physical value of the momentum $q \neq 0$, we have that only a few values of L can be considered for this fit.